Central European Journal of Energetic Materials
ISSN 1733-7178; e-ISSN 2353-1843

Cent. Eur. J. Energ. Mater. 2020, *17*(1): 119-141; DOI 10.22211/cejem/119352
Article is available in PDF-format, in colour, at:
http://www.wydawnictwa.ipo.waw.pl/cejem/Vol-17-Number1-2020/CEJEM_01066.pdf

Research paper

Mechanical Properties of HTPE/Bu-NENA Binder and the Kinetics of Bu-NENA Evaporation

Shen Yuan[1,2], Yunjun Luo[1,2,*]

[1] *School of Materials Science and Engineering, Beijing Institute of Technology, Beijing 100081, China*
[2] *Key Laboratory for Ministry of Education of High Energy Density Materials, Beijing Institute of Technology, Beijing 100081, China*
* *E-mail:* yjluo@bit.edu.cn

Abstract: The correlation between the mechanical properties of hydroxyl-terminated polyether (HTPE)/*N*-butyl-*N*-(2-nitroxyethyl)nitramine (Bu-NENA) binders with different plasticization ratios (*pl/po*), varied from 0.9 to 1.5, have been studied. The very early stage of evaporation of Bu-NENA from the HTPE/Bu-NENA binder, with a *pl/po* ratio of 1.2, has been investigated. The results revealed that the *pl/po* ratio has strong influences on the mechanical properties. When the *pl/po* ratio was 1.2, the mechanical properties of the HTPE/Bu-NENA binder were satisfactory, the maximum tensile strength and the elongation at break being 2.39 MPa and 93.27%, respectively. The evaporation rate constant of Bu-NENA from HTPE/Bu-NENA binder with a *pl/po* ratio of 1.2 increased from $0.31 \cdot 10^{-5}$ to $2.32 \cdot 10^{-5}$ s^{-1} as the temperature was increased from 50 to 90 °C. The value of the activation energy of evaporation was 51.47 kJ/mol and its pre-exponential factor was $6.14 \cdot 10^{2}$ s^{-1}.

Keywords: hydroxyl-terminated polyether, HTPE, *N*-butyl-*N*-(2-nitroxyethyl)nitramine, Bu-NENA, mechanical properties, cross-linking network structure, evaporation

1 Introduction

Solid propellants are expected to resist various stresses during storage, transportation, ignition and flight. Any damage caused to a solid propellant under the aforementioned stresses can cause serious deterioration in the performance of the solid rocket motor [1]. As a consequence, the mechanical properties of a solid propellant are some of its most important physical properties [2-4]. Differing from other types of propellants, a composite solid propellant is a multiphase system composed of a polymer binder matrix and solid fillers. Under stress processes, the polymer binder matrix (mass fraction 10-20%) of a composite solid propellant often determines its mechanical properties [1]. The cross-linked network structure of the polymer binder matrix will be the major origin of the mechanical properties of a composite solid propellant [5, 6]. The cross-linked network structure not only includes the chemical cross-linked network, such as the cross-linked density (V_e) and the molecular weight between the cross-linked points (M_c), but can also form the physical cross-linked network due to hydrogen bonding (H-bonded) interactions and microphase separation. It can, more directly, reveal trends in the mechanical properties of the binder. Mao *et al*. [7, 8] studied the effect of cross-linked network structures on the mechanical properties of an hydroxyl-terminated epoxyethane/tetrahydrofuran random copolymer (PET) and polyfuctional isocyanate (N-100) binder, where the results showed that the H-bonded effect and the chemical cross-linked structure of the PET/N-100 binder were related to the curing parameter (R value). Ma *et al*. [9] enhanced the mechanical properties of glycidyl azide polymer (GAP)/toluene diisocyanate (TDI) binder by improving its cross-linked network.

Hydroxyl-terminated polyether (HTPE) is a new type of binder, developed to meet the requirements of insensitive munition (IM) properties and high performance. The ether bonds in the HTPE molecular chain allow good flexibility. An HTPE binder can exhibit favorable low temperature mechanical properties and good compatibility with energetic nitrate plasticizers [10, 11]. The dielectric coefficient of electrostatic insulation of an HTPE binder is several orders of magnitude higher than that of the currently used HTPB binder, so that the possibility of electrostatic ignition and the risk of detonation during the use and production of an HTPE propellant are greatly reduced [12, 13].

One kind of smokeless HTPE propellant has a maximum strength of 1.05 MPa and an elongation at break of 36% at room temperature, and the elongation at break is slightly reduced to 35% when the temperature is lowered to –40 °C [14]. With another kind of HTPE propellant, its maximum

strength is 2.2 MPa and the elongation at break is 57% at –40 °C [15]. For better processing and IM properties, energetic plasticizers compatible with an HTPE binder can be used [16, 17]. *N*-butyl-*N*-(2-nitroxyethyl) nitramine (Bu-NENA) is a typical energetic plasticizer that could improve the properties of propellants because it confers good plasticization by the nitrate ester groups. In addition, Bu-NENA has low mechanical sensitivity. Using Bu-NENA to plasticize an HTPE propellant will create the current development requirements for IM properties [18]. However, evaporation of Bu-NENA will reduce the physical, thermal and mechanical properties of a propellant. This will ultimately cause the propellant to crack at stress-concentration points and the grains of the propellant will become weakened [19]. This is the reason why evaporation of Bu-NENA from composite solid propellant is of such importance. In previous reports, Tompa *et al*. [20] found that the size and shape of a propellant both directly affect the rate of evaporation. Zhao *et al*. [21], using isothermal thermogravimetry (TG), calculated that the enthalpy of Bu-NENA evaporation from an NC/Bu-NENA propellant was 69.75 kJ/mol. The evaporation of Bu-NENA follows a zero-order reaction model at a very early stage of evaporation, while the power law of the evaporation rate changes with time. The addition of Bu-NENA to an HTPE binder will inevitably have an influence on the regularity of the HTPE molecular chain and the cross-linked network of the HTPE binder, which in turn will affect the mechanical properties of the HTPE binder. Therefore, before working on an HTPE propellant, it is important that fundamental research on the mechanical properties of an HTPE/Bu-NENA binder and evaporation of Bu-NENA from such a binder should be explored. Unfortunately, there is almost no publicly available information on the details of such studies.

In the present work, Fourier transform infrared spectroscopy (FT-IR) and low field nuclear magnetic resonance spectroscopy (LF-NMR) were used to explore the H-bonded interactions, including microphase separations and the chemical cross-linked network of HTPE/Bu-NENA binders with different plasticization ratios (*pl/po*), respectively. The integrities of the networks of these HTPE/Bu-NENA binders were evaluated. Moreover, uniaxial tensile experiments were used to study the mechanical properties of these energetic binders. Finally, the evaporation of Bu-NENA from a HTPE/Bu-NENA binder was investigated, including the evaporation kinetics, using isothermal TG. Our work hopefully will provide guidance on the mechanical properties of HTPE/Bu-NENA binders and fundamental results on evaporation of Bu-NENA from HTPE/Bu-NENA binders.

2 Materials and Methods

2.1 Materials

Hydroxyl-terminated polyether (HTPE) prepolymer with an average molecular weight of 3600 g/mol and hydroxyl group (–OH) content of 0.48 mmol/g (Scheme 1 shows the molecular structure of the HTPE prepolymer), and *N*-butyl-*N*-(2-nitroxyethyl)nitramine (Bu-NENA) were purchased from Liming Research Institute of Chemical Industry, Henan, China. Trimethylolpropane (TMP) with a hydroxyl group content of 23.60 mmol/g, toluene diisocyanate (TDI) with an isocyanate group (–NCO) content of 11.48 mmol/g, and the curing catalyst triphenyl bismuth (TPB, 0.5%) dissolved in dioctyl sebacate (DOS), were purchased from Beijing Chemical Works. HTPE, Bu-NENA and TMP were dried in a vacuum for 2 days at 60 °C before use.

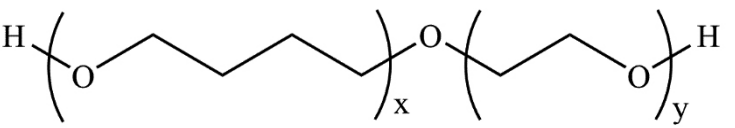

Scheme 1. The molecular structure of the HTPE prepolymer

2.2 Preparation of HTPE/Bu-NENA Binders

The curing parameter (*R* value) represents the equivalence ratio of –NCO and –OH groups, which has a significant effect on the mechanical properties of a polyurethane binder. The *R* value is theoretically set as 1.0. Thus, excellent mechanical properties can be obtained by the polyurethane binder. Considering side effects, the *R* value should be appropriately adjusted according to the practical situation. The final *R* value was set to 1.7, which is equivalent to an excess of –NCO.

HTPE, TMP, Bu-NENA and TDI were weighed precisely according to the proportions in Table 1, and thoroughly mixed in an appropriate beaker. A 0.3% solution of TPB was then added to the beaker and stirred until evenly mixed. After continuous stirring for 20 min, the mixture was cast into a polytetrafluoroethylene mold to form a film of approximately 3-4 mm thickness and evacuated for 2 h at 40 °C in order to remove residual bubbles and moisture. Subsequently, the HTPE/Bu-NENA binder was cured at 60 °C for 7 days. HTPE/Bu-NENA binders with different plasticization ratios (*pl/po*, varying from 0.9 to 1.5) were prepared.

Table 1. The proportions of Bu-NENA, HTPE, TMP and TDI in the prepared HTPE/Bu-NENA binders

pl/po	Bu-NENA [wt.%]	HTPE [wt.%]	TMP [wt.%]	TDI [wt.%]
0.9	47.37	28.18	5.00	19.45
1.0	50.00	26.77	4.75	18.48
1.1	52.38	25.50	4.52	17.60
1.2	54.55	24.34	4.31	16.80
1.3	56.52	23.28	4.13	16.07
1.4	58.33	22.31	3.96	15.40
1.5	60.00	21.42	3.80	14.78

2.3 Measurements

The hydrogen bonding (H-bonded) interactions and microphase separation studies were conducted using Fourier transform infrared spectroscopy (FT-IR, Nicolet 8700, Thermo Fisher Scientific, USA). The chemical cross-linked network structures were analyzed by low field nuclear magnetic resonance spectroscopy (LF-NMR, VTMR20-010V-T, Niumai Corporation, China). The mechanical properties were tested using a universal testing machine (AGS-J, Shimadzu, Japan). The thermal properties were analyzed by non-isothermal thermogravimetry (TG, TGA/DSC1SF/417-2, Mettler Toledo, Switzerland) and differential scanning calorimetry (DSC, HP DSC 2+, Mettler Toledo, Switzerland), with N_2 flow (40 cm^3/min) over the temperature range 50-550 °C at a heating rate of 10 °C/min. The evaporation was tested by isothermal thermogravimetry (TG, TGA/DSC1SF/417-2, Mettler Toledo, Switzerland) with N_2 flow (40 cm^3/min) over the temperature range 50-90 °C; each sample weight was around 5 mg, having a thickness of 3-4 mm. The Bu-NENA content inside each HTPE/Bu-NENA binder was measured by high performance liquid chromatography (HPLC, LC-20AD, Shimadzu, Japan), each specimen weight was around 20 mg with a thickness of 3-4 mm, methanol (25 μL) as the solvent was added to the specimen for 24 h and then extracted.

3 Results and Discussion

3.1 Mechanical properties of the HTPE/Bu-NENA binders

3.1.1 Hydrogen bonding interactions and microphase separations

The hydrogen bonding (H-bonded) interactions in an HTPE/Bu-NENA binder are mainly formed by carbonyl (–C=O) and imino (–NH) groups on hard

segments [22]. These H-bonds cause aggregation between the hard segments, thus forming microphase separations that contribute to the mechanical properties of the binder. Assuming that H-bonds in the HTPE/Bu-NENA binders are formed, the FT-IR spectroscopic absorptions of the carbonyl groups will shift to a lower wavenumber [9].

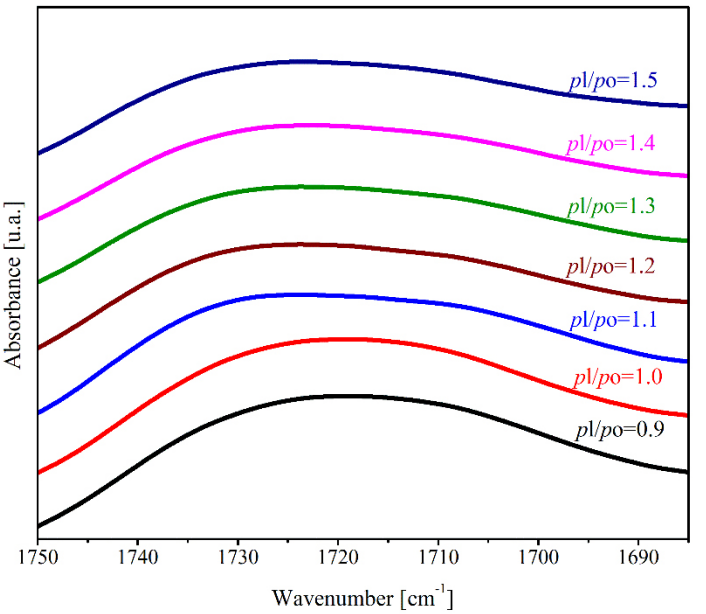

Figure 1. The FT-IR spectra of the carbonyl groups in HTPE/Bu-NENA binders

Consequently, the H-bonded interactions within the HTPE/Bu-NENA binders with various plasticization ratios (*pl/po*) were studied through their FT-IR spectra. Figure 1 shows the FT-IR spectra of carbonyl groups in HTPE/Bu-NENA binders with different *pl/po* ratios. The strong spectral absorption band of the carbonyl group is in the broad range of 1750 to 1690 cm^{-1}. With increasing *pl/po* ratio, the FT-IR spectrum of the carbonyl group absorption shifts to a higher wavenumber, indicating that the addition of Bu-NENA affects the formation of H-bonds between the carbonyl and imino groups. The FT-IR peaks of the carbonyl groups are assigned to the ordered and free carbonyl groups. The more ordered carbonyl groups can form stronger H-bonded interactions. However, the overlap of free and ordered carbonyl group absorptions makes it hard to analyze the H-bonded interactions in the binders. In order to distinguish the overlapped carbonyl group peaks, we took the second derivative of the FT-IR

absorption to determine the accurate spectral absorption peaks and used multi-peak Gaussian fitting to calculate the relative areas and proportions of these two different carbonyl groups in the HTPE/Bu-NENA binders. The second derivative results are shown in Figure 2.

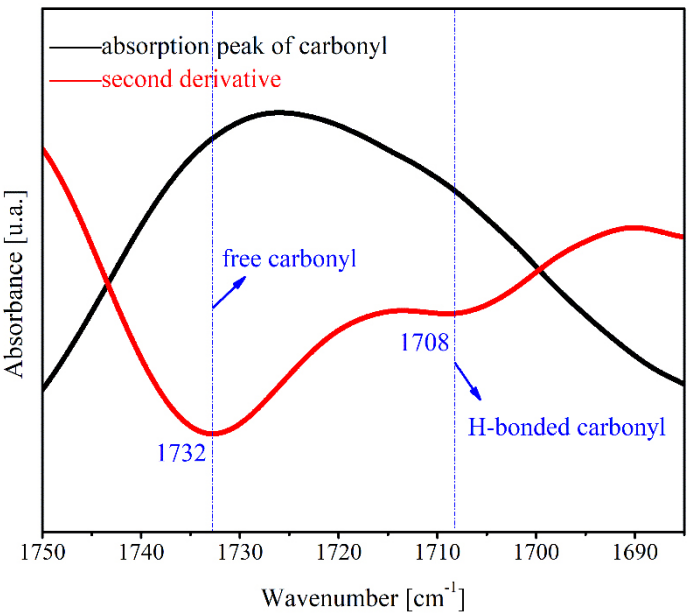

Figure 2. The second derivative FT-IR spectra of the carbonyl groups

The second derivative FT-IR spectrum of the carbonyl groups in Figure 2 shows two peak troughs located at 1732 and 1708 cm^{-1}, which correspond respectively to free carbonyl and H-bonded carbonyl groups in the carbonyl group region [22]. Multi-peak Gaussian fitting of the carbonyl groups can then be achieved according to the determined different carbonyl group absorption positions. The results are shown in Figure 3 and Table 2.

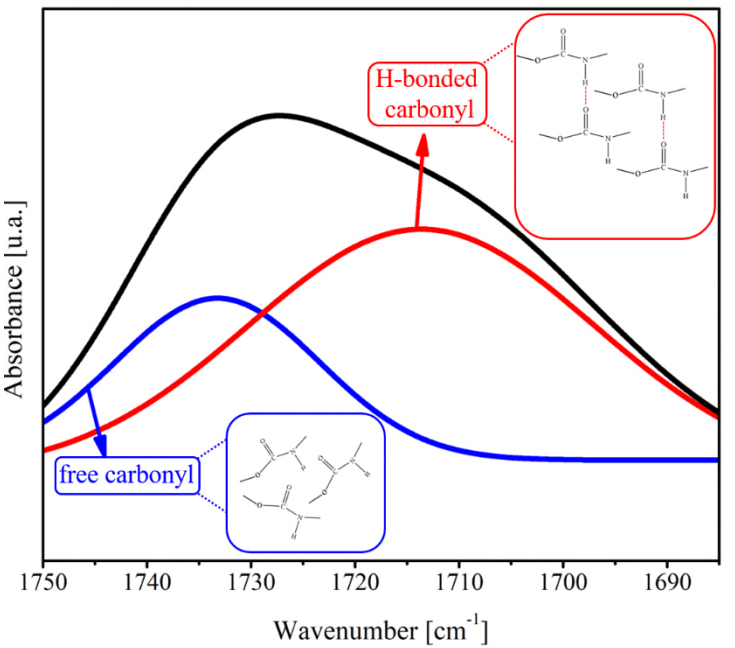

Figure 3. The multi-peak Gaussian fitting of FT-IR spectra of the carbonyl groups

Table 2. The absorption peak areas of the carbonyl groups and H-bonded proportions of HTPE/Bu-NENA binders with different *pl/po* ratios

pl/po ratios	Absorption peak areas [u.a.]		H-bonded proportions [%]
	Free carbonyl (1732 cm^{-1})	H-bonded carbonyl (1708 cm^{-1})	
0.9	0.3622	0.2996	45.27
1.0	0.3214	0.2517	43.92
1.1	0.3877	0.2677	40.85
1.2	0.2557	0.1778	41.01
1.3	0.3025	0.1926	38.90
1.4	0.3491	0.2061	37.12
1.5	0.1884	0.0910	32.57

Table 2 shows that the H-bonded proportions of the HTPE/Bu-NENA binders with *pl/po* ratios increasing from 0.9 to 1.5, changed from 45.27 to 32.57%, which demonstrated that H-bonded interactions obviously exist in the binders. However, the H-bonded proportions have a decreasing trend with increasing Bu-NENA content. Because Bu-NENA as a plasticizer

is not going to be involved in the curing reaction, and an increase in its content will reduce the concentration of carbamate (–NHCOO–) groups formed by the curing reaction. Thus, the reduction of carbonyl and imino groups in the carbamate groups is not conductive to the formation of intermolecular and intramolecular H-bonds. At the same time, the attenuation of H-bonded interactions causes the ordered arrangement between hard segments to be destroyed, and the emergence of this situation is contrary to the formation of microphase separations. Microphase separation is similar to filler reinforcement and also acts as a physical cross-linked point for soft segments, which is beneficial for the mechanical properties of the binders. The addition of Bu-NENA increases the distance between molecular chains and makes the arrangement of molecular segments capable of forming H-bonds loose. Therefore, as the *pl/po* ratios is increased, the H-bonded interactions and the microphase separations of the HTPE/Bu-NENA binders are weakened, which is not beneficial for improving the mechanical properties of the binders.

3.1.2 Chemical cross-linked network structures

Chemical cross-linking can increase the relationship between the polymer molecular chains, making the molecular chains less prone to relative slippage. The chemical cross-linked network structures of HTPE/Bu-NENA binders with diverse *pl/po* ratios were investigated by LF-NMR. The LF-NMR test results for the binders, including the cross-linked density (V_e) and the molecular weight between the cross-linked points (M_c), are shown in Table 3.

Table 3. The chemical cross-linked network parameters of the HTPE/Bu-NENA binders

pl/po ratios	V_e ($\cdot 10^{-4}$) [mol/cm^3]	M_c ($\cdot 10^3$)
0.9	1.902	5.258
1.0	1.840	5.435
1.1	1.707	5.857
1.2	1.626	6.151
1.3	1.567	6.382
1.4	1.534	6.520
1.5	1.495	6.691

Table 3 reveals clearly that the V_e value of the HTPE/Bu-NENA binders is reduced continuously as the *pl/po* ratio is increased. The addition of Bu-NENA as a micromolecule plasticizer has a diluting effect on the cross-linked points in the HTPE/Bu-NENA binders. The stronger dilution effect leads to a lower

relative content of cross-linked points as the *pl/po* ratio is increased continuously from 0.9 to 1.5. Moreover, Bu-NENA also lowers the concentration of the curing reactive groups that are involved, so for the HTPE/Bu-NENA binders it becomes more difficult to form the chemically cross-linked network. Due to these reasons, the V_e values of the HTPE/Bu-NENA binders become reduced with increasing Bu-NENA content. By contrast, the M_c values of the HTPE/Bu-NENA binders show a totally opposite trend, compared to the V_e values. This behaviour occurs because the ability to bind the cross-linked molecular chains becomes weakened, and the increase in a molecular chain's activity allows it to be further extended.

3.1.3 Integrity of the cross-linked network structures

Physical and chemical cross-linking will affect the network structure of an HTPE/Bu-NENA binder, and the integrity of the cross-linked network directly impacts on the mechanical properties of the binder itself. Therefore, the degree of integrity of an HTPE/Bu-NENA binder network was studied by comparing the calculated and actual elastic modulus according to the rubber elasticity statistical theory of cross-linked structures [23]. The shear modulus (G) and the cross-linked network parameters have the following interrelations:

$$G = NkT = \frac{N_A \rho kT}{M_c} = \frac{\rho RT}{M_c} \tag{1}$$

where G is the shear modulus; N is the total chain number in the cross-linked network; k is Boltzmann's constant; T is the absolute temperature [K]; N_A is Avogadro's constant; ρ is the density of the cured network; R is the molar gas constant.

This theory assumes that both ends of each chain in the cross-linked network are connected at the cross-linking point, and all of the chains contribute to the modulus in deformation, which is an idealized case. However, it is impossible to create such an ideal situation in the cross-linked structure because other network structures actually exist [8]. The H-bonded interactions, which can form physical entanglements of molecular chains interspersed with each other, create favorable contributions to the modulus and the strength of the binder. The formation of enclosed rings, pendant groups and free chains on the same molecular chains belonging to defects have an adverse influence on the mechanical properties of the binder [24]. Hence, it is difficult to calculate and count the exact interactions between physical entanglements and individual defects. In order to solve this problem, an approach was considered to reflect the degree of integrity of an HTPE/Bu-NENA binder cross-linked

network by introducing a correction factor (D) into Equation 1. Thus Equation 1 can be rewritten as:

$$\lambda G = E = \lambda V_e RT + D \quad (2)$$

where E is the elastic modulus; λ is the Poisson ratio; D is the correction factor. The correction factor D is on behalf of the relative contributions to the modulus of H-bonded interactions and defects of the binder. A positive value of the correction factor D indicates that the influence of H-bonded interactions and physical entanglements on the modulus of the binder is more effective than that of the defects, and *vice versa*. The results of the correction factor D for the HTPE/Bu-NENA binders are shown in Table 4 for further analysis.

Table 4. The cross-linked network integrity of the HTPE/Bu-NENA binders

pl/po ratio	*E* [MPa]	*D* [MPa]
0.8	4.93	1.03
0.9	4.50	0.93
1.0	4.09	0.80
1.1	3.98	0.81
1.2	3.85	0.79
1.3	3.72	0.75
1.4	3.15	0.59
1.5	2.31	0.32

Table 4 demonstrates that the correction factor D for all of the HTPE/Bu-NENA binders is positive, indicating that the integrity of the cross-linked network of the HTPE/Bu-NENA binders is maintained under favorable conditions. Since the functionality of TMP is uniform, defects such as enclosed rings can hardly be formed after the curing reaction. Besides, the end groups on both TMP and HTPE are highly reactive primary hydroxyl groups, so the probability of forming pendant groups and free chains is reduced after the curing reaction. However, the correction factor D of the HTPE/Bu-NENA binders reveals a decreasing tendency as the *pl/po* ratio is increased. This is because the addition of Bu-NENA reduces the relative concentration of the curing reactive groups, leading to a decline in the degree of curing. In addition, the H-bonded interactions also demonstrate a reduction with increasing quantity of Bu-NENA, while Bu-NENA weakens the action of physical entanglement in the HTPE/Bu-NENA binders. The decrease in cross-linked density demonstrates that the HTPE/Bu-NENA binders have difficulty

in forming chemically cross-linked networks as the content of Bu-NENA is increased. H-bonded interactions and chemical cross-linking both contribute to the integrity of the cross-linked network structure. Finally, the correction factor *D* of the HTPE/Bu-NENA binders decreases as the amount of Bu-NENA is increased, but is still maintained at beneficial values. The conclusions derived from this analysis suggests that a favorable integrity of cross-linked network structure exists in the HTPE/Bu-NENA binders.

3.1.4 Mechanical properties

As an energetic plasticizer, Bu-NENA will dilute the concentrations of the curing reactive groups and reduce the interactions between the molecular chains. The addition of Bu-NENA and the changes in its content also have significant influences on the mechanical properties of a polyurethane binder. Thus, a universal testing machine was used to analyze the mechanical properties of the HTPE/Bu-NENA binders as a function of different *pl/po* ratios. The stress-strain curves in the uniaxial tensile testing of the HTPE/Bu-NENA binders and the corresponding results of maximum tensile strength (σ_m) and elongation at break (ε_b) are given in Figure 4 and Table 5, respectively. From the curves depicted in Figure 4, it is clear that the nature of the curve from the HTPE/Bu-NENA binders does not change with increasing *pl/po* ratio, and the elongation at maximum tensile strength and the elongation at break are almost coincident. However, the binders have lower strength, elongation or initial slope with higher *pl/po* ratios.

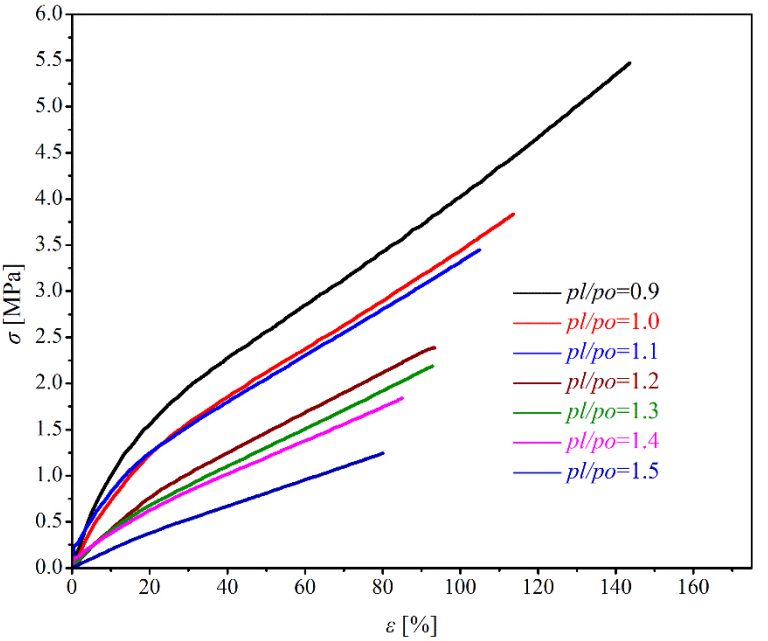

Figure 4. The uniaxial tensile curves of HTPE/Bu-NENA binders

Table 5. The σ_m and ε_b of the HTPE/Bu-NENA binders

pl/po ratio	σ_m [MPa]	ε_b [%]
0.9	5.47	143.60
1.0	3.83	113.66
1.1	3.45	104.95
1.2	2.39	93.27
1.3	2.19	92.76
1.4	1.84	84.97
1.5	1.24	79.95

The physical and chemical cross-linked interactions are inherently capable of improving the strength of the binders. However, the concentrations of the curing reactive groups become diluted and the interactions between the molecular chains are reduced as the *pl/po* ratio becomes higher with higher Bu-NENA contents. These conditions will reduce the H-bonded interactions in the binders, such as microphase separations and physical entanglements along with chemical cross-linked densities. Hence, in the cases where the physical and chemical cross-linked interactions are both weakened, the strength

of the binders are continuously lowered. For elongation of the HTPE/Bu-NENA binders, although the presence of Bu-NENA is beneficial to the molecular weight between the cross-linked points and the activities of the molecular chains, the integrity of the cross-linked network structures of the binders becomes incomplete. At this point, an increase in the molecular weight between cross-linked points can no longer offset the effects of deteriorations in the curing networks on elongation, so the elongation at break is reduced.

One conclusion derived from these analyses is that relatively satisfactory mechanical properties exist in HTPE/Bu-NENA binders; when the *pl/po* ratio is 1.2, the σ_m is 2.39 MPa and ε_b is 93.27%, which can meet the requirements of subsequent process performance.

3.2 Bu-NENA evaporation from a HTPE/Bu-NENA binder

The evaporation of Bu-NENA will affect the physical, chemical, thermal and mechanical properties of binders. This is the reason why the evaporation of Bu-NENA from an HTPE/Bu-NENA binder should be taken into consideration. Based on the analyses given above, we selected the HTPE/Bu-NENA binder with a *pl/po* ratio of 1.2 for studying the evaporation of Bu-NENA.

3.2.1 Thermal properties of the HTPE/Bu-NENA binder

Before studying the evaporation of Bu-NENA, the non-isothermal TG curve of the studied HTPE/Bu-NENA binder, along with the non-isothermal TG curve of the HTPE binder without plasticizer were measured. The results are shown in Figure 5.

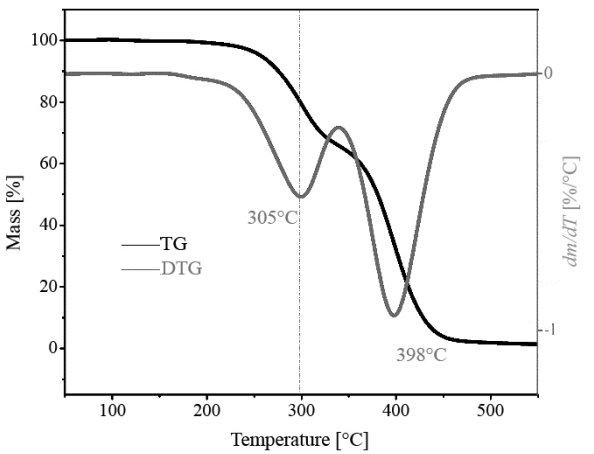

(a)

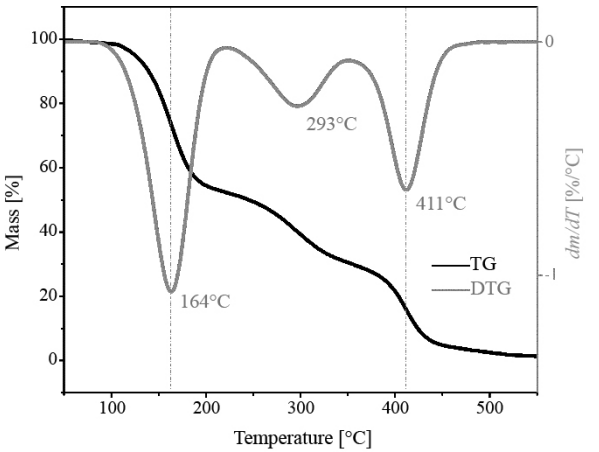

(b)

Figure 5. The non-isothermal TG curves of (a) HTPE binder, and (b) HTPE/Bu-NENA binder

The thermal decomposition of the HTPE binder has two apparent mass loss stages, starting at 223 °C and following on to the next at 340 °C, which correspond to the decomposition of carbamate in the HTPE binder and decomposition of the HTPE polyether backbone, respectively. However, the HTPE/Bu-NENA binder shows three mass loss stages. The first one appears within the temperature range 92 to 218 °C, predominantly accompanied by the evaporation or decomposition of Bu-NENA. The remaining two stages are similar to those of the decomposition of the HTPE binder. It may be observed from Figure 5, that in the case of the HTPE binder a noticeable mass loss is observed at 200 °C, while in the case of the HTPE/Bu-NENA binder it occurs at 92 °C, as demonstrated by the differential scanning calorimetry (DSC) curve of Bu-NENA in Figure 6. There is no noticeable exothermic process for Bu-NENA below 170 °C. This reveals that the mass loss beginning at 92 °C in Figure 5(b) is caused by Bu-NENA evaporation from the HTPE/Bu-NENA binder, not its decomposition. This also means that the evaporation of Bu-NENA can be completely separated from the decomposition of HTPE/Bu-NENA binder if the temperatures of the isothermal TG experiments are considerably lower than the decomposition temperature of HTPE/Bu-NENA. To exclude the effects of the decomposition of the HTPE/Bu-NENA binder, the isothermal TG analysis was conducted below 90 °C.

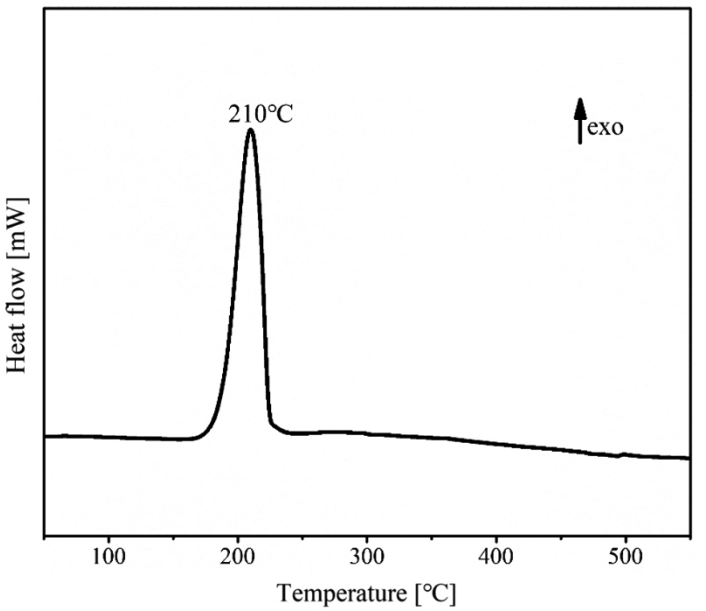

Figure 6. The DSC curve of Bu-NENA

3.2.2 Kinetics of Bu-NENA evaporation from the HTPE/Bu-NENA binder

To conduct a systematic study on the evaporation of Bu-NENA, the HTPE/Bu-NENA binder was subjected to isothermal TG analysis at temperatures between 50 and 90 °C, and the results are shown in Figure 7. In order to ascertain that Bu-NENA loss was the main reason for the mass loss in Figure 7, the Bu-NENA content of the HTPE/Bu-NENA binder isothermally aged for 14 h at different temperatures was measured by HPLC. A comparison of Bu-NENA loss from the HTPE/Bu-NENA binder as measured by HPLC and the isothermal TG result is given in Table 6.

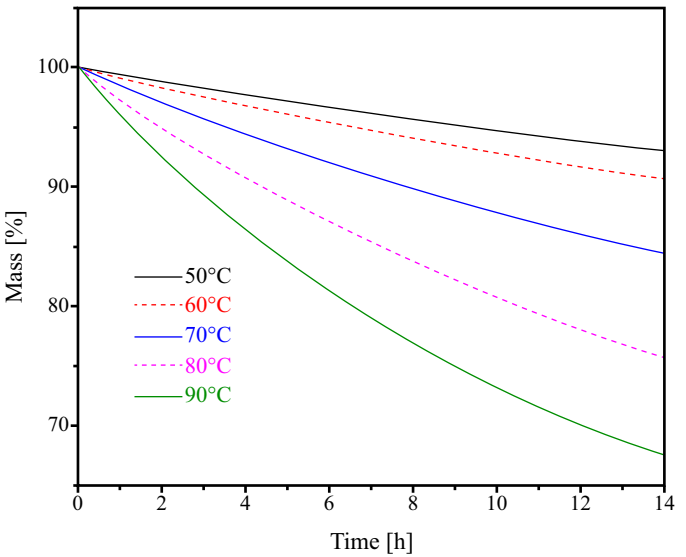

Figure 7. The isothermal TG curves of the HTPE/Bu-NENA binder at different temperatures

Table 6. HPLC for Bu-NENA loss in an HTPE/Bu-NENA binder at different temperatures after isothermal ageing for 14 h

Temperature [°C]	HPLC for Bu-NENA loss [%]	TG for mass loss [%]
50	7.09	7.03
60	11.87	9.42
70	15.15	15.68
80	29.33	24.34
90	31.94	32.34

The results of Bu-NENA loss obtained by HPLC were quite consistent with the results from isothermal TG, suggesting that the mass loss in the isothermal TG was mainly caused by evaporation of Bu-NENA. Therefore, the kinetic parameters of Bu-NENA evaporation could be derived from the mass loss-time curves for the HTPE/Bu-NENA binder in Figure 7. The mass loss-time data for the HTPE/Bu-NENA binder were converted to the degree of conversion (α) *vs.* time by Equation 3 [25].

$$\alpha = \frac{m_t - m_o}{m_f - m_o} \tag{3}$$

where m_o is the onset sample mass, m_f is the final sample mass, and m_t is the instantaneous sample mass. A is calculated using the final sample mass m_f as the sample mass after complete evaporation of Bu-NENA, so the difference value of m_o and m_f is 54.55%.

We observed that the plasticizer molecules on the surface of the HTPE/Bu-NENA binder were evaporated first. During the progress of the evaporation, the inner plasticizer molecules of the HTPE/Bu-NENA binder must migrate or diffuse through the binder matrix to its surface before the Bu-NENA can evaporate further. During the period of plasticizer evaporation, the Bu-NENA content decreases, and it also migrates or diffuses from the inner region to the surface, which affects the characteristics of evaporation. Therefore, the evaporation of Bu-NENA is more complicated and its rate becomes lower with increasing time. To avoid the effects of migration or diffusion of Bu-NENA, the conversion rate *vs.* α ($d\alpha/dt$ *vs.* α) of the HTPE/Bu-NENA binder is shown in Figure 8.

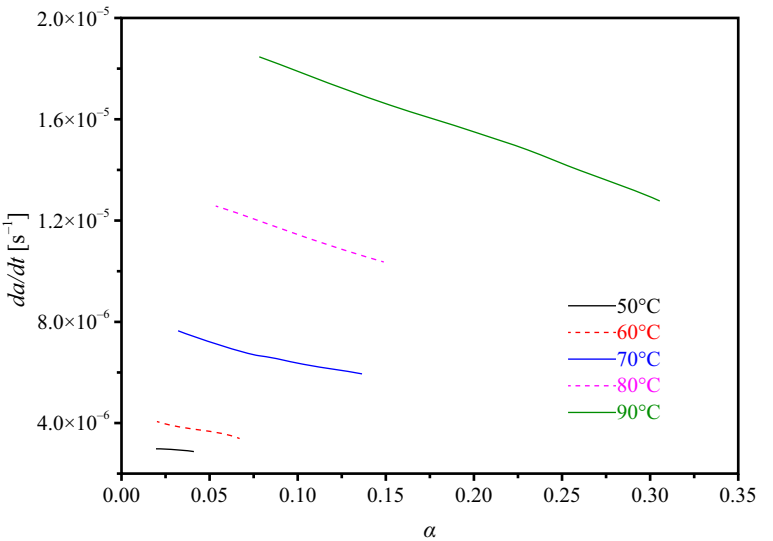

Figure 8. Conversion rate vs. conversion curves of the HTPE/Bu-NENA binder at different temperatures

The evaporation of Bu-NENA conforms to the basic kinetic equation, as Equation 4 [26].

$$\frac{d\alpha}{dt} = k_{vap} f(\alpha) \tag{4}$$

where k_{vap} is the evaporation rate constant, $f(\alpha)$ is a function that can represent the relation of the rate of conversion on the conversion. $f(\alpha)$ can be usually simplified as $(1 - \alpha)^n$, just like the homogeneous kinetics of gases. In this way, the variation of the apparent activation energy under varied experimental conditions can be explored [25] and the simplified nonlinear equation is shown as Equation 5.

$$\frac{d\alpha}{dt} = k_{vap}(1 - \alpha)^n \tag{5}$$

The evaporation process of Bu-NENA from the HTPE/Bu-NENA binder can be described as the *n*-th order nonlinear function of Equation 5. The exponent *n* depends on the size and shape of the HTPE/Bu-NENA binder, but the evaporation rate constant k_{vap} is only temperature dependent and will not change with the size and shape. Therefore, the size and shape, including the weight of the sample, must be kept the same in the analysis of each term. In this way, the evaporation rate constant k_{vap} can be achieved by fitting to Equation 5, and these results are listed in Table 7.

Table 7. The evaporation rate constants of HTPE/Bu-NENA binders at different temperatures

Sample	k_{vap} ($\cdot 10^{-5}$) [s^{-1}]				
	50 °C	60 °C	70 °C	80 °C	90 °C
HTPE/Bu-NENA	0.31	0.46	0.92	1.61	2.32

The values in Table 7 show that the evaporation rate constant becomes larger with increasing temperature. To further understand the evaporation behaviour of the HTPE/Bu-NENA binder, we calculated the activation energy of evaporation (E_{vap}) according to the Arrhenius plot of $\ln(k_{vap})$ *vs.* $1/T$ (T is temperature in K), as shown in Figure 9.

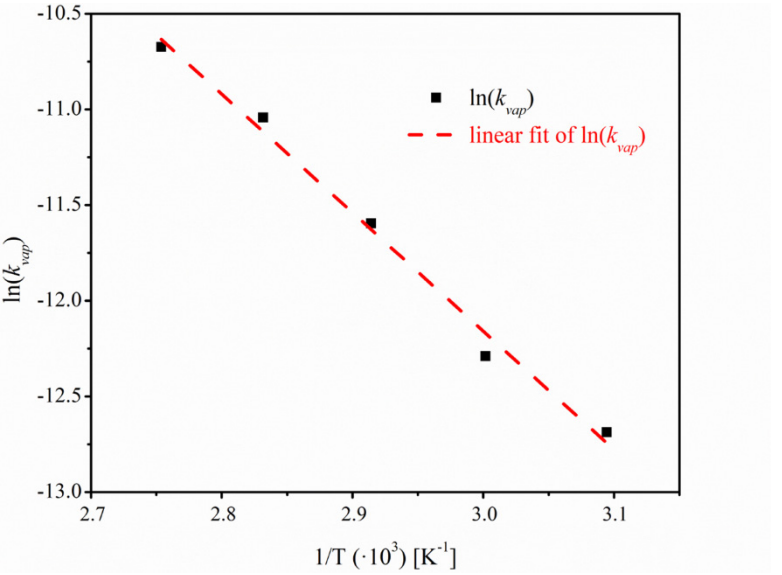

Figure 9. Arrhenius plots of weight loss rate of the HTPE/Bu-NENA binder (equation of the line is $y = -6191x + 6.42$)

The value of E_{vap} obtained for the HTPE/Bu-NENA binder was 51.47 kJ/mol, with a pre-exponential factor (A_{vap}) of $6.14 \cdot 10^2$ s^{-1}. k_{vap} is not only related to E_{vap} (the energy barrier that the plasticizer needs to overcome) but also to the frequency factor. However, the frequency factor is associated with the entropy, which is influenced by molecular structure. Bu-NENA has a long molecular chain and its molecular structure is loose and asymmetric, which can inhibit Bu-NENA evaporation [19].

4 Conclusions

HTPE/Bu-NENA binders with various *pl/po* ratios were prepared in this study. The mechanical properties of these HTPE/Bu-NENA binders, and the evaporation of Bu-NENA from the binder with a *pl/po* ratio of 1.2, were investigated.

The addition of Bu-NENA diluted the concentration of the reactive groups and reduced the interactions between molecular chains. As the content of Bu-NENA was increased, the H-bonded interactions and the microphase separations of the HTPE/Bu-NENA binders were weakened. At the same time the cross-linked densities were reduced and the integrity of the cross-linked

network structure was damaged. All of these factors caused the mechanical properties of HTPE/Bu-NENA to deteriorate with increasing *pl/po* ratios. Considering the subsequent energy content and the processing performance of the solid propellant, a *pl/po* ratio in a HTPE/Bu-NENA binder was chosen as 1.2. At this point, the mechanical properties of an HTPE/Bu-NENA binder with a *pl/po* ratio of 1.2 can meet the requirements; the maximum tensile strength and the elongation at break of the binder were 2.39 MPa and 93.27%, respectively. The corresponding H-bonded proportion was 41.01% and the cross-linked density was $1.626 \cdot 10^{-4}$ mol/cm^3.

The evaporation of Bu-NENA from the HTPE/Bu-NENA binder with a *pl/po* ratio of 1.2 complied with the power law of evaporation rate with time. The evaporation rate constant of Bu-NENA increased from $0.31 \cdot 10^{-5}$ to $2.32 \cdot 10^{-5}$ s^{-1} as the temperature was increased from 50 to 90 °C. The activation energy of evaporation was 51.47 kJ/mol, and its pre-exponential factor was $6.14 \cdot 10^{2}$ s^{-1}. The evaporation of Bu-NENA followed zero-order kinetics at the initial stage.

The results for the mechanical properties of HTPE/Bu-NENA binders with various *pl/po* ratios and the kinetics of Bu-NENA evaporation could be helpful for the optimization of mechanical properties, processing temperature and storage conditions for binders or solid propellants.

References

[1] Tan, H.M. The *Chemistry and Technology of Solid Rocket Propellant*. 1st ed, Beijing Institute of Technology Press, Beijing, **2015**, pp. 186; ISBN 978-7-56-409714-1.
[2] Duncan, E.S.; Margetson, J. A Nonlinear Viscoelastic Theory for Solid Rocket Propellants Based on a Cumulative Damage Approach. *Propellants, Explos., Pyrotech*. **1998**, *23*(2): 94-104.
[3] Li, G.C.; Wang, Y.F.; Jiang, A.M.; Yang, M.; Li, J.F. Micromechanical Investigation of Debonding Processes in Composite Solid Propellants. *Propellants, Explos., Pyrotech*. **2018**, *43*(5): 642-649.
[4] Zhang, L.; Zhi, S.J.; Shen, Z.B. Research on Tensile Mechanical Properties and Damage Mechanism of Composite Solid Propellants. *Propellants, Explos., Pyrotech.* **2018**, *43*(3): 234-240.
[5] Kohga, M. Mechanical Characteristics and Thermal Decomposition Behavior of Polytetrahydrofuran Binder Using Glycerol Propoxylate (M_n = 260) as Crosslinking Agent. *Propellants, Explos., Pyrotech* **2017**, *38*(3): 366-371.
[6] Liu, J.R.; Song, X.J.; Yang, Y. Study on the Adjustment Method of NEPE Propellant Binder Matrix Structure. *J. Solid Rocket Technol.* **2010**, *33*(1): 72-76.

[7] Mao, K.Z.; Luo, Y.J.; Xia, M. Effect of Polyethylene Glycol on Curing Kinetic and Mechanical Properties of Polyether of Ethylene Oxide and Tetrahydrofuren/ Polyfunctional Isocyanate N-100 Binder System. (in Chinese) *Polym. Mater. Sci. Eng. (Chengdu, China)* **2013**, *29*(10): 34-37.
[8] Mao, K.Z.; Ma, S.; Luo, Y.J. Crosslinking Network Structure Integrity of PET/N-100 Binder System. *Chin. J. Energ. Mater.* **2015**, *23*(10): 941-946.
[9] Ma, S.; Li, Y.J.; Li, G.P.; Luo, Y.J. Research on the Mechanical Properties and Curing Networks of Energetic GAP/TDI Binders. *Cent. Eur. J. Energ. Mater*. **2017**, *14*(3): 708-725.
[10] Zhang, W.B.; Fang, X.D.; Zhu, X.Z.; Fan, W.W. Synthesis and Mechanical Properties of Poly(tetrahydrofuran)-poly(butadiene)-poly(tetrahydrofuran) Triblock Copolymer. *J. Solid Rocket Technol.* **2015**, *2*(5): 251-255.
[11] Wang, C.D.; Luo, Y.J.; Xia, M. Synthesis of HTPE and Properties of HTPE Elastomers. *Chin. J. Energ. Mater.* **2011**, *19*(5): 518-522.
[12] Kai, F.; Tokerud, D.; Biserod, H.; Orbekk, E.; Tenden, S.; Kaiserman, M.; Rodack, M.; Spate, W.; Winetrobe, S.; Royce, B.; Wallace, S. The Hypervelocity Anti-Tank Missile Development Program; Rocket Motor Design and Development. *AIAA/ASME/SAE/ASEE Joint Propulsion Conference & Exhibit, 41st*, Tucson, AZ, USA, **2005**, 4172.
[13] Kaiserman, M.; Rodack, M.; Spate, W.; Winetrobe, S.; Royce, B.; Wallace, S.; Biserod, H.; Fossumstuen, K.; Tokerud, D. An Overview of the Hypervelocity Anti-Tank Missile (HATM) Development Program. *AIAA/ASME/SAE/ASEE Joint Propulsion Conference & Exhibit, 41st*, Tucson, AZ, USA, **2005**, 4171.
[14] Fletcher, W.G.; Comfort, T.S. Updates on HTPE Propellants Service Life. *Insensitive Munitions Energ. Mater. Technol. Symp.,* Bristol, UK, **2006**, 9.
[15] Yan, D.Q.; Xu, D.D.; Shi, J.G. A Review of Solid Propellant Binder HTPE Development and Its Molecular Design Philosophy. *J. Solid Rocket Technol.* **2009**, *32*(6): 644-649.
[16] Shi, X.B.; Pang, W.Q.; Wei, H.J. Research Progress and Development Trends of Insensitive Propellant. *Chem. Propellants Polym. Mater.* **2007**, *5*(2): 24-28.
[17] Wang, W.X.; Xue, J.Q.; He, W.G.; Zhou, J.Y.; Yu, H.C.; Shang, B.K. Performance and Application of Bu-NENA Energetic Plasticizer. *Chem. Propellants Polym. Mater.* **2014**, *12*(1): 1-22.
[18] Damse, R.S. Evaluation of Energetic Plasticizers for Solid Gun Propellant. *Def. Sci. J.* **2008**, *58*(1): 86-93.
[19] Cartwright, R.V. Volatility of NENA and Other Energetic Plasticizers Determined by Thermogravimetric Analysis. *Propellants, Explos., Pyrotech.* **2010**, *20*(2): 51-57.
[20] Tompa, A.S. Thermal Analysis of Liquid and Solid Propellants. *J. Hazard. Mater*. **1980**, *4*(1): 95-112.
[21] Zhao, B.B.; Zhang, T.F.; Wang, Z.; Sun, S.X.; Ge, Z.; Luo, Y.J. Kinetics of Bu-NENA Evaporation from Bu-NENA/NC Propellant Determined by Isothermal Thermogravimetry. *Propellants, Explos., Pyrotech.* **2017**, *42*(3): 253-259.
[22] Yilgor, I.; Yilgor, E.; Guler, I.G.; Ward, T.C.; Wilkes, G.L. FTIR Investigation

of the Influence of Diisocyanate Symmetry on the Morphology Development in Model Segmented Polyurethanes. *Polymer* **2006**, *47*(11): 4105-4114.
[23] Fried, E. An Elementary Molecular-Statistical Basis for the Mooney and Rivlin-Saunders Theories of Rubber Elasticity. *J. Mech. Phys. Solids* **2002**, *50*(3): 571-582.
[24] Kramer, O. Contribution of Entanglements to Rubber Elasticity. *Polymer* **1979**, *20*(11), 1336-1342.
[25] Šesták, J. Study of the Kinetics of the Mechanism of Solid-State Reactions at Increasing Temperatures. *Thermochim. Acta* **1971**, *3*(1): 1-12.
[26] Sućeska, M.; Mušanić, S. M.; Houra, I.F. Kinetics and Enthalpy of Nitroglycerine Evaporation from Double Base Propellants by Isothermal Thermogravimetry. *Thermochim. Acta* **2010**, *510*(1): 9-16.

Received: May 10, 2019
Revised: March 24, 2020
First published online: March 26, 2020